Desalination and Water Treatment
www.deswater.com
doi: 10.5004/dwt.2020.25141

182 (2020) 155–167
April

Treatment of lead contaminated water using lupin straw: adsorption mechanism, isotherms and kinetics studies

Hanie Hashtroudi[a,b]

[a]*School of Engineering, Joondalup Campus, Edith Cowan University, 270 Joondalup Drive, Joondalup WA 6027, Australia, Tel. +61392148444; email: hhashtroudi@swin.edu.au*
[b]*Faculty of Science, Engineering and Technology, Swinburne University of Technology, Hawthorn, VIC 3122, Australia*

Received 29 October 2018; Accepted 9 November 2019

ABSTRACT

Lupin straw has been studied for its efficiency as a low-cost natural adsorbent to remove dissolved Pb^{2+} ions from synthetic wastewater. Experiments were carried out within this study to understand the effect of various environmental conditions such as contact times, pHs, adsorbent dosages, and adsorbate concentrations. The surface characteristics of lupin straw were investigated utilizing energy dispersive X-ray spectroscopy, Fourier transform infrared spectroscopy, and scanning electron microscopy devices. The highest percentage removal of Pb(II) was found to be 98.4% at 5 mg/L initial metal concentration. The breakthrough curve and exhaustive capacity of the adsorbent were determined to be 10.98 and 20.16 mg/g, respectively. Experimental results were evaluated using different isotherm equations developed by Langmuir, Freundlich, Harkins–Jura, Redlich–Peterson, and Halsey. Among these, the Freundlich and Halsey isotherms had a higher correlation coefficient ($r^2 > 0.998$). The pseudo-first-order, pseudo-second-order, intra-particle diffusion, Elovich, and fractional power kinetic models were utilized to investigate the dynamic mechanism of lead adsorption over time.

Keywords: Agricultural waste; Lupin straw; Isotherms; Kinetics; Pb(II) adsorption

1. Introduction

The world's main water resources are being polluted by undesirable organic and inorganic wastes that have been released into the environment because of the advance of civilization and rapid industrialisation. The presence of toxic contaminants such as heavy metals can damage both the ecosystem and the human body [1]. Although some heavy metals are essential parts of the biochemical process in the human body, the required level of consumption is on a micro or macro scale [2]. Drinking contaminated water can be harmful to human health even at low concentration levels, and water quality improvement is therefore one of the most significant environmental issues in the world.

Toxic heavy metal ions are mostly found in urban stormwater run-off and industrial wastewaters. They are produced as a result of activities such as mining and quarrying, electronic assembly planting, battery recycling planting, and etching operations [3]. Industrial wastewaters are discharged directly or indirectly into the environment and the pollutants they contain are transferred to primary water resources through surface run-off. Lead is one of the most harmful heavy metals for human health and it can remain in the body for years. Pb(II) can be found in urban stormwater runoff because of its presence in gasoline. This causes contamination of the soil near streets and drainage ways. Pb(II) can also accumulate in aquatic sediments and find its way through aqueous solutions as a result. Prolonged exposure

to Pb has been shown to cause various life-threatening conditions such as several forms of cancer, kidney damage, central nerve system damage, brain damage, dermatitis, dizziness, and liver problems [4]. Lead has a half-life of about 600–3,000 d where most of the inhaled Pb is accumulated in the bones [5].

Several conventional physical, chemical, and biological techniques have been used to remove toxic lead ions from aqueous solutions, including membrane filtration [6,7], oxidation [8,9], ion exchange [10,11], reverse osmosis [12,13], electrolysis [14], chemical precipitation [15], water filtration [16,17], gutter system and hydrodynamic separators [18], magnetic base methods [19–22], and adsorption techniques [23–26]. Although these methods are commonly used for Pb(II) removal, in some cases the use of these techniques is virtually precluded due to costs being prohibitively high as well as issues with efficiency at low Pb(II) concentrations [27,28]. Although adsorption is a feasible process to remove dissolved Pb(II) from aqueous solutions, the cost of using conventional media (e.g., activated carbon and resin) render this process cost inhibitive for the treatment of large quantities of contaminated water [24,29,30].

The use of economical adsorbents to reduce the cost of treatment has been intensified in recent years. Attention has focused on various natural agro-waste adsorbents such as fruit peel [31,32], fruit shells [33], nut shells [34–36], husks and straw [25,37], and seeds [38,39] as low-cost adsorbents which are highly efficient and mostly available in large quantities [35,40–42].

This study provides a methodology for eliminating Pb(II) ions from synthetic wastewater using lupin straw as a local agricultural waste of Western Australia. To the best of the authors' knowledge, the literature does not include any information about using lupin straw as an adsorbent to remove contaminants from water and more particularly no study has been reported concerning the use of lupin straw as an adsorbent to remove Pb(II) ions from aqueous solutions. This paper, therefore, represents a novel contribution to the research area. The present study highlights the fact that lupin straw is highly effective as an economical, biodegradable and environmentally clean adsorbent to remove Pb(II) from aqueous solutions. The main advantage of using raw lupin straw as adsorbent is that it minimises the use of chemicals during the water treatment process. In contrast, chemical and thermal treatments are generally expensive, where energy intensive processes and the possibility of releasing unwanted by-products from chemically treated adsorbents into water may create a need for further remediation procedures.

The present study tested the efficiency of lupin straw for the removal of lead in low concentrations from synthetic wastewater. The effects of experimental factors such as initial pH, contact time, adsorbent dosage, and adsorbate concentration were investigated. The obtained experimental data were then validated using different isotherm and kinetic models to investigate the adsorption process of Pb(II) ions onto the surface of the adsorbents. This research demonstrated that lupin straw is highly effective as economical, biodegradable and environmentally clean adsorbent for the removal of Pb(II) from contaminated water.

2. Theory

2.1. Adsorption isotherm and kinetic models

In this study, the Langmuir, Freundlich, Harkins–Jura, Redlich–Peterson, and Halsey isotherm models are used to investigate the sorption equilibrium for lead removal from aqueous solutions using lupin straw. Linear and non-linear forms of all isotherm equations are presented in Table 1. Isotherm studies describe the surface of the

Table 1
Linear and non-linear forms of isotherm equations

Isotherm models	Non-linear form	Linear form
Langmuir	$q_e = \frac{b_l C_e Q_0}{1 + b_l C_e}$	$\frac{C_e}{q_e} = \frac{C_e}{Q_0} + \frac{1}{b_l Q_0}$
Freundlich	$q_e = K_f C_e^{\frac{1}{n_f}}$	$\log(q_e) = \log(K_f) + \frac{1}{n_f}\log(C_e)$
Harkins–Jura	$q_e = \left(\frac{A_H}{B_H - \log C_e}\right)^{\frac{1}{2}}$	$\frac{1}{q_e^2} = \left(\frac{B_H}{A_H}\right) - \left(\frac{1}{A_H}\right)\log C_e$
Redlich–Peterson	$q_e = \frac{A_R C_e}{1 + B_R C_e^{\beta}}$	$\ln\left(A_R \frac{C_e}{q_e} - 1\right) = \beta \ln C_e + \ln B_R$
Halsey	$q_e = \left(\frac{k_H}{\ln(C_e)}\right)^{\frac{1}{n_H}}$	$\ln q_e = \left[\left(\frac{1}{n_H}\right)\ln k_H\right] - \left(\frac{1}{n_H}\right)\ln C_e$

q_e: experimental equilibrium adsorption capacity (mg/g); C_e: equilibrium adsorbate concentration (mg/L); b_1, Q_0: Langmuir constants; K_f, n_f: Freundlich constants; A_H, B_H: Harkins–Jura constants; A_R, B_R, β: Redlich–Peterson constants; k_H, n_H: Halsey constants.

adsorbent as homogeneous (Langmuir isotherm) and heterogeneous (Freundlich, Harkins–Jura, and Halsey isotherms). The Redlich–Peterson isotherm is a combination of the Langmuir and Freundlich isotherms incorporating three elements. Consequently, this isotherm is applicable for either heterogeneous or homogeneous surfaces of the adsorbent. The Langmuir isotherm is a model based on the assumption that all the active sites for the adsorption process have an equal affinity for binding. In the Freundlich isotherm model, stronger binding sites are usually occupied at the beginning of the adsorption process and the affinity for binding then decreases over time [43–45]. In the Langmuir isotherm, the constant values of b_1 and Q_0 (the maximum monolayer adsorption capacity) can be obtained from the intercept and slope of the plot C_e/q_e vs. C_e respectively. Likewise, in the Freundlich isotherm the constant values of n_f and K_f can be calculated from the intercept and slope of the plot $\log(q_e)$ vs. $\log(C_e)$, respectively.

The possibility of a multilayer adsorption process assumed in the Harkins–Jura and Halsey isotherms can be explained by the presence of heterogeneous pore distribution and heteroporous solids, respectively [46,47]. The Halsey isotherm constants k_H and n_H can be determined from the slope and intercept of the plot of $\ln q_e$ vs. $\ln C_e$, respectively. Constants A_H and B_H of the Harkins–Jura equation can be determined from the plot $1/q_e^2$ vs. $\log C_e$. The mixed adsorption process in the Redlich–Peterson isotherm does not follow ideal monolayer adsorption. The Redlich–Peterson constant parameters A_R and β can be obtained from the intercept and slope of plotting $\ln(A_R C_e/q_e - 1)$ vs. $\ln C_e$, respectively.

The physical and chemical properties of the adsorbent influence the adsorption process. Thus, there are different kinetic models proposed to evaluate reaction pathways over time and investigate whether the process is based on physisorption or chemisorption interactions. In this study, five different kinetic models have been applied to investigate the adsorption process in different adsorbate concentrations over time. Table 2 shows the non-linear and linear forms of different kinetic equations [48–53].

After considering initial and final boundary conditions ($t = 0 - t$ and $q_t = 0 - q_t$), the non-linear kinetic equations become linear. The constant parameters of each kinetic model can be obtained from the slope and intercept of the linear form plots.

3. Materials and methods

3.1. Material preparation

The lupin straw used in the present study was collected from a local farm in Perth, Western Australia. The straw was thoroughly washed with water several times to remove dust and dirt, followed by three thorough washes with deionized water to remove lighter soluble contaminants. The washed lupin straw was dried in an oven at 100°C for 24 h. Thereafter, the dried adsorbent was ground and sieved to retain a particle size of less than 200 μm. The size of the adsorbent was measured using a Mastersizer (Malvern 3000). Table 3 demonstrates the results of this measurement, which shows that more than 90% of the lupin straw particles were under 190 μm. The adsorbate solutions were prepared through a

Table 3
Mastersizer size measurement result

Span	3.483
Uniformity	1.025
Specific surface area (m^2/kg)	215.1
D [3,2] (μm)	27.9
D [4,3] (μm)	78.1
D (10) (μm)	12.8
D (50) (μm)	50.9
D (80) (μm)	129
D (90) (μm)	190

Table 2
Non-linear and linear forms of different kinetic models

Kinetic models	Non-linear form	Linear form	Plot for linear form
Pseudo-first-order	$\frac{dq_t}{dt} = k_f(q_e - q_t)$	$\log(q_e - q_t) = \log(q_e) - \frac{k_f}{2.303}t$	$\log(q_e - q_t)$ vs. time
Pseudo-second-order	$\frac{dq}{dt} = k_S(q_e - q_t)^2$	$\frac{t}{q_t} = \frac{1}{k_S q_e^2} + \frac{1}{q_e}t$	$\frac{t}{q_t}$ vs. time
Intra-particle diffusion		$q_t = K_i t^{\frac{1}{2}} + C_i$	q_t vs. $t^{\frac{1}{2}}$
Elovich	$q_t = \frac{1}{\beta}\ln(1 + \alpha\beta t)$	$q_t = \beta\ln(t) + \alpha$	q_t vs. $\ln(t)$
Fractional power	$q_t = \varepsilon t^{\omega}$	$\ln(q_t) = \ln(\varepsilon) + \omega\ln(t)$	$\ln(q_t)$ vs. $\ln(t)$

q_t: Amount of lead adsorbed by lupin straw at time "t"; K_f: constant value of pseudo-first-order kinetic model; K_S: constant value of the pseudo-second-order; K_i (mg/g $min^{1/2}$) and C_i (mg/g): intra-particle diffusion rate constant values; α and β: constant values of the Elovich kinetic model; ε and ω: constant values of the fractional power kinetic model.

serial dilution procedure using high purity stock standard lead (1,000 mg/L) solution.

The required amount of stock solution was transferred to the volumetric flask containing deionized water and hydrochloric acid (HCL) each time. The prepared adsorbate solution was diluted to the required different concentrations before starting the experiment. Hydrochloric acid (0.1 mol/L) and sodium hydroxide (0.1 mol/L) solutions were used for pH adjustment [54]. All these chemicals were obtained from Agilent Technologies Australia and Merck Pty limited, Australia. The pH of the solutions was measured by a pH meter (Rowescience WP-90Z).

3.2. Adsorbent characterization and dissolved Pb(II) analysis

The concentration of lead ions during the experiment was analysed using microwave plasma atomic emission spectroscopy (Agilent 4200 MP-AES). The surface characterization of the adsorbent was determined using scanning electron microscopy (SEM, JEOL JSM-6000). The chemical composition of the lupin straw surface was investigated by energy dispersive X-ray spectroscopy (EDS, DX200s). Fourier transform infrared (FTIR, PerkinElmer UTAR Spectrum two) was used within a range of 4000–400 cm^{-1} to investigate functional groups on the adsorbent surface.

3.3. Batch adsorption experiment

In the present study the batch adsorption experiments were performed in 100 mL flasks. After adding the necessary amount of adsorbent, the prepared 100 mL solutions were shaken by a temperature-controlled mechanical shaker (RATEK OM11 digital orbital shaking incubator) at 200 rpm. The temperature was kept constant at 23°C during all the batch experiments. Different pHs, contact times, adsorbent dosages and adsorbate concentrations were tested during the experiment. The pH of the mixtures was adjusted by adding 0.1 M HCl and 0.1 M NaOH solutions. After stirring the samples for the predetermined desired contact time, the mixtures were filtered out and the aqueous phase of every sample was analyzed for its Pb(II) concentration using MP-AES. Different experimental conditions such as initial adsorbent dosages (10–50 g/L), lead concentrations (5–15 mg/L), pHs (4–8), and contact times (5–120 min) were examined to determine maximum adsorption capacity of lupin straw. The equilibrium contact time was determined after testing different predetermined time intervals. The adsorption capacity of lupin straw was calculated from following equation:

$$q_e = \frac{\left(C_i - C_e\right)V}{D_i} \tag{1}$$

where q is the adsorption capacity of the adsorbent (mg/g), C_i and C_e are the initial and equilibrium concentrations of adsorbate (mg/L), V is the volume of the contaminated solution (L), and D_i is the mass of adsorbent (g). The percentage of Pb(II) removal was also calculated as follows:

$$\text{Lead removal}\left(\%\right) = \left[\frac{C_i - C_e}{C_i}\right] \times 100 \tag{2}$$

4. Results and discussion

4.1. SEM–EDS analysis

The spatial properties of the adsorbent surface have a remarkable influence on the initial stages of the adsorption process. Thus, in this study the SEM images were captured to compare the surface texture, roughness, and the morphology of the lupin straw before and after the experimentation process.

The SEM images of lupin straw before and after the experiment are shown in Figs. 1a and b, respectively. The rough surface morphology of lupin straw (Fig. 1a) facilitates the adsorption process and shows strong potential for adsorbate ions to be extracted from the solution. After the experiment, the surface of the lupin straw became smoother as shown in Fig. 1b. Based on the morphological features, it can be concluded that the morphological characterization of lupin straw enables it to keep possession of lead ions.

The EDS study identified the elemental composition of the lupin straw, as shown in Fig. 1c, and clearly demonstrated that lupin straw has a high percentage of carbon (88.27%) and oxygen (11.73%). This makes lupin straw a suitable adsorbent material.

4.2. Fourier transform infrared spectroscopy analysis

Fourier transform infrared spectroscopy (FTIR) analysis is an effective technique to identify the different functional groups that are responsible for the adsorption process on the adsorbent surface. Fig. 2 shows the FTIR spectra of the lupin straw before and after the adsorption process in the range of 4,000 to 400 cm^{-1}. As expected, the results show that lupin straw is a cellulosic based plant. Normally, the intramolecular hydrogen bond in cellulose occurs around 3,340 cm^{-1} [55,56]. Therefore, as shown in Fig. 2, a strong adsorption broad band around 3,334 and 3,321 cm^{-1} of lupin straw before and after experimentation can be assigned to the overlapping of the different stretching modes of the hydroxyl group from the phenol groups of the lignin and cellulose of the lupin straw and N–H symmetric stretching vibration. The peak at 2,917 cm^{-1} is related to eminent asymmetric C–H stretch bond where the carbon is sp^3-hybridized [32,57]. The bands at 1,735 and 1,728 cm^{-1} are assigned to C=O aldehyde carboxyl groups while the other peaks in the fingerprint region at 1,369; 1,263; 1,155; and 1,051 cm^{-1} are attributed to C–H bending, C–O–C asymmetric stretching, and C–O valence vibrations of carbohydrate groups, respectively [58–60]. The absorption peaks at 1,595 and 1,263 cm^{-1} are assigned to aromatic C=C and C–O bending vibrations [61]. The bend at 1,031 cm^{-1} is ascribed to C–N stretching vibration. The peak position of the band at 1,505 cm^{-1} is assigned to C=C aromatic symmetrical stretching while the peak at 1,159 cm^{-1} is related to non-symmetric bridge C–O–C vibration [62]. The bend at 897 cm^{-1} can be attributed to the amorphous region on the lupin straw surface. Another broad band around 559 cm^{-1} could be assigned to out-of-plane O–H bending vibrations [63]. According to Fig. 2, no remarkable differences were observed in the FTIR spectra of lupin straw before and after the adsorption process.

The energy of hydrogen bonds for the OH stretching bands was obtained using following equation [64,65]:

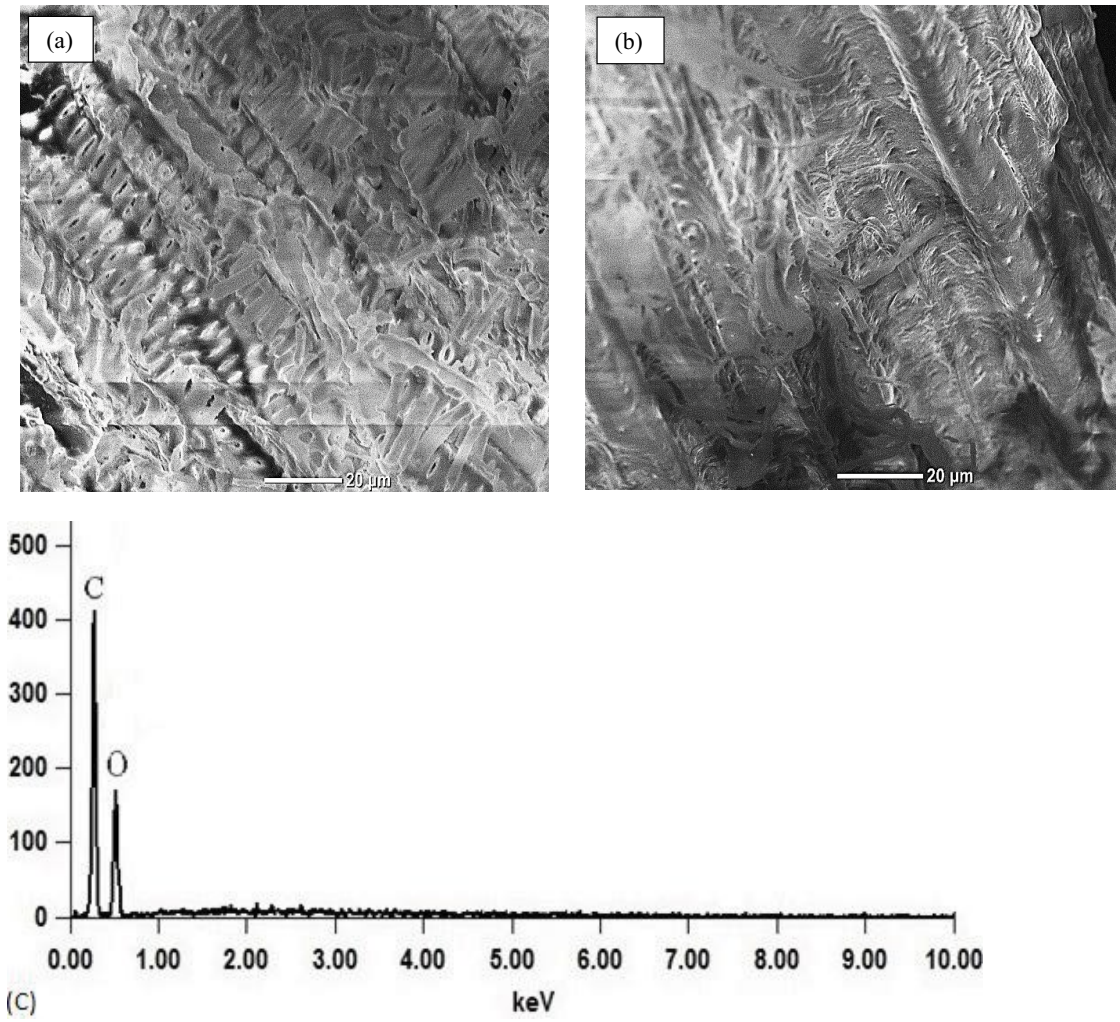

Fig. 1. SEM images of lupin straw before the experiment (a) and after the experiment (b), EDS spectra of lupin straw (c)

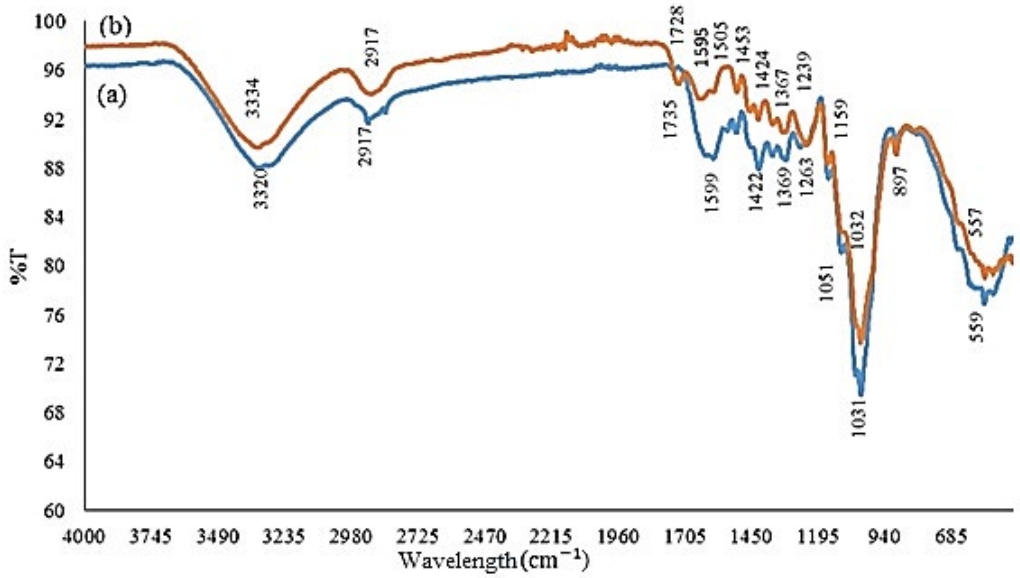

Fig. 2. Fourier transform infrared spectra of lupin straw before (a) and after (b) the adsorption.

$$E = \frac{\left(\nu_{OH} - \nu_{H}\right)}{K\nu_{OH}} \quad (3)$$

where K is a constant value ($1/K$ = 262.5 kJ); ν_{OH} is the standard frequency of the free OH groups which is taken to be 3,650 cm^{-1}; and ν_{H} is the infrared spectrum frequency of the OH groups observed in the lupin straw. In addition, the hydrogen bond distance (R_H) was calculated from the following equations [65]:

$$\Delta\nu_{H} = 4430 \times \left(2.84 - R_{H}\right) \quad (4)$$

$$\Delta\nu_{H} = \nu_{M} - \nu_{H} \quad (5)$$

where ν_H is the stretching infrared spectrum frequency of lupin straw that was observed from the experiment and ν_M is the monomeric stretching infrared spectrum frequency of the OH bond (3,600 cm^{-1}). The calculated hydrogen bond energies and distances for lupin straw before and after experimentation are presented in Table 4. The lower energy value of the hydrogen bond in lupin straw after the experiment could be due to the amount of adsorbed water during the experiment. The higher energy value of the lupin straw before the adsorption may illustrate a higher number of intramolecular hydrogen bonds in cellulose. According to the results presented in Table 4, a lower hydrogen bond distance is associated with a higher energy value in the lupin straw before the experiment.

Some intramolecular hydrogen bonds between phenolic groups in lignin and cellulose may cause a reduction in the hydrogen bond distance [59].

4.3. Effect of pH on lead uptake

A series of experiments were performed at different pH values varying from 4 to 8 by adding 1 g of lupin straw into 100 mL prepared lead solutions at three different concentrations (5, 10, and 15 mg/L) at a temperature of 23°C. All the experiments were carried out at an agitation speed of 200 rpm for 120 min. The pH of the mixtures was adjusted by adding 0.1 M HCl and 0.1 M NaOH solutions. The initial pH of the mixture has a remarkable influence on the adsorption process, so the percentage removal of the adsorbate is dependent on the pH value. Due to the existence of H^+ at acidic medium, the surface of the lupin straw became protonated so the attraction between the positively charged surface and Pb^{2+} decreased which resulted in low removal efficiency as shown in Fig. 3 [22]. By increasing the pH from 4 to 5.5, the Pb(II) removal efficiency rose slightly: 95% to 98.4% at 5 mg/L lead concentration, 94.3% to 97% at 10 mg/L lead concentration, and 93.2% to 95.7% at 15 mg/L lead concentration. As shown in Fig. 3, Pb(II) uptake was found to be the highest at pH 5.5 and decreased with the rise of the pH from 5.5 to 6. For lead concentration of 5 mg/L, the percentage removal of lead ions decreased from 98.4% at pH 5.5 to 95% at pH 6.0. This pattern was repeated for different adsorbate concentrations: 97% to 94% at 10 mg/L lead concentration, and 95.7% to 93% at 15 mg/L lead concentration. When the pH rose from 6.0 to 7.0, the adsorption rate increased slightly: 94.7% to 95% at 5 mg/L lead concentration, 94% to 94.4% at 10 mg/L lead concentration, and 93% to 93.3% at 15 mg/L lead concentration. While increasing the pH from 7.0 to 8.0 resulted in a small decrease of adsorption rate: 95% to 93.9% at 5 mg/L lead concentration, 94.4% to 92.9% at 10 mg/L lead concentration, and 93.3% to 92.3% at 15 mg/L lead concentration. The highest percentage removal of Pb^{2+} ions was obtained at pH 5.5. The electrostatic interactions between the oppositely charged functional groups on the lupin straw surface and Pb^{2+} ions, explain the increased uptake of lead ions at pH 5.5.

The adsorption of lead as a metal is a complex process that is affected by various factors, such as surface charge, micro-precipitation, physical surface characteristics, and the number of hydroxyl groups on the adsorbent surface. The optimum pH value for lead removal by lupin straw was found at 5.5, and 98.4% of the lead ions were removed when the adsorbate concentration was 5 mg/L. Due to the obtained results, the rest of the experiments were carried out at pH 5.5.

4.4. Effect of contact time at different initial metal concentrations on lead uptake

The effect of contact time was investigated by performing a series of experiments at different contact times from 5 to 120 min for various initial metal concentrations (5, 10, and 15 mg/L) at 23°C and pH 5.5. The equilibrium time was found

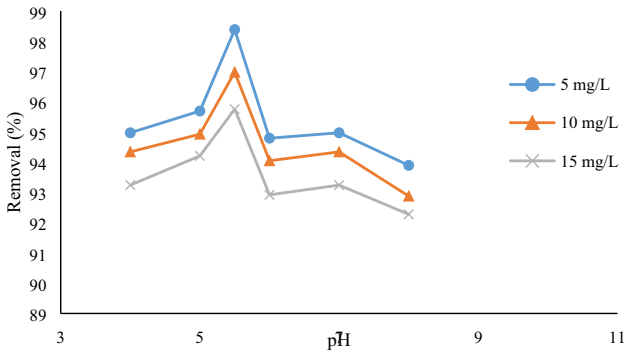

Fig. 3. Effect of pH on lead removal by lupin straw in different initial metal concentrations.

Table 4
Hydrogen bond energies and distances for lupin straw before and after experiment

Material	OH groups wavelength (cm^{-1})	Energy (kJ)	Distance (Å)
Lupin straw before the experiment	3,320	23.7328	2.776
Lupin straw after the experiment	3,334	22.7260	2.779

to be 60 min and the maximum uptakes of Pb(II) were calculated to be 98.4%, 96.98%, and 95.75% after 60 min at initial metal concentrations of 5, 10, and 15 mg/L, respectively (Fig. 4). The high extraction efficiency could be due to the presence of some anionic functional groups such as carboxylate ($–COO^-$), hydroxyl (–OH), and phenoxide ($–C_6H_5O^-$) groups on the lupin straw surface. This facilitates interactions between anions and Pb^{2+} ions as metal cations [66]. The adsorption rate was rapid at the beginning of the experiment, as 90.67%, 89.27%, and 86.42% of lead ions were removed after 5 min at initial adsorbate concentrations of 5, 10, and 15 mg/L, respectively. The rate of the adsorption became slower in the later stages of the experiment, moving toward saturation at 60 min. The equilibrium time was independent of the initial lead concentration. The quick initial sorption rate might be explained by the large quantity of active sites located on the adsorbent surface: these play an important role in the sorption process. The process continued with the slower rate due to the saturation of active sites until the equilibrium was reached [35,66].

4.5. Breakthrough curve and exhaustive capacity

Determining the breakthrough capacity through column experiment is important as it directly affects the efficiency, feasibility, and cost effectiveness of the adsorbent for the removal of the adsorbate in the adsorption process [67]. 1 g lupin straw was compacted into a column (6 mm internal diameter and 24 mm bed height) with glass wool support. 1,000 mL of lead solution with initial concentration of 5 mg/L (C_i) was then infiltrated into the column at a flow rate of 1 mL/min. The effluent was collected in 50 mL at the beginning and then in 50 mL fractions. The MP-AES analysis was utilized to determine the residual Pb(II) concentrations (C_e) of each fraction. The breakthrough curve was obtained by plotting C_e/C_i vs. volume of effluent. The exhaustive capacity was found when the C_e/C_i = 1. Fig. 5 shows that 150 mL of the effluent containing 5 mg/L Pb(II) could be passed through the column without detecting lead ions when 1 g of the lupin straw was used. The breakthrough and exhaustive capacities were found to be 10.98 and 20.16 mg/g, respectively.

4.6. Adsorption equilibrium studies

4.6.1. Adsorption isotherm study

The isotherm constant parameters were calculated from the intercepts and slope of the linear plots of Fig. 6. All the isotherm parameters at different adsorbent dosage are presented in Tables 5 and 6. In the Langmuir isotherm, the values of R_L were calculated as follows:

$$R_L = \frac{1}{1 + b_L C_i} \tag{6}$$

where b_L is the Langmuir constant (L/mg), C_i is the initial concentration of lead in solution (mg/L). The $R_L > 1$ indicates that the adsorption process is unfavourable while $0 < R_L < 1$ indicates a favourable process. Likewise, $R_L = 0$ and $R_L = 1$ demonstrate irreversible and linear adsorption processes, respectively. In this study the values of R_L were in the range of 0 to 1, which reflects a desirable adsorption process for the removal of lead using lupin straw.

As shown in Table 5, both the Langmuir and the Freundlich isotherm models achieved a good fit, but correlation coefficient values (r^2) for the Freundlich isotherm were higher than the Langmuir isotherm which implies that the Freundlich isotherm was more applicable for the lead removal process using lupin straw. The Freundlich isotherm indicates a heterogeneous adsorbent surface and multilayer adsorption process [44]. This isotherm is based on the assumption that the stronger binding sites are taken first and the affinity for binding reduces as a greater number of sites are occupied [68].

The Freundlich constant K_f represents the amount of adsorbate adsorbed onto the adsorbent surface for a unit equilibrium concentration. The calculated value of $0 < 1/n_f < 1$ from the intercept of the plot $\log(q_e)$ vs. $\log(C_e)$ in the Freundlich isotherm, indicates the high uptake ability of lupin straw at all adsorbent dosages.

According to Table 6, although the experimental data fits well with both the Redlich–Peterson and Halsey isotherm

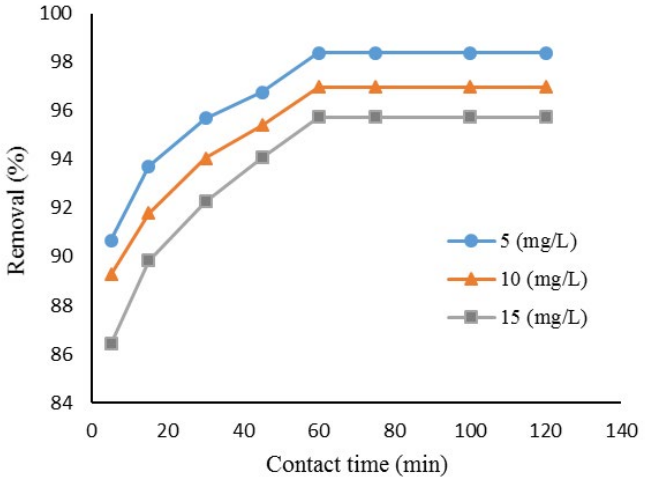

Fig. 4. Effect of contact time on lead removal by lupin straw at different initial metal concentrations

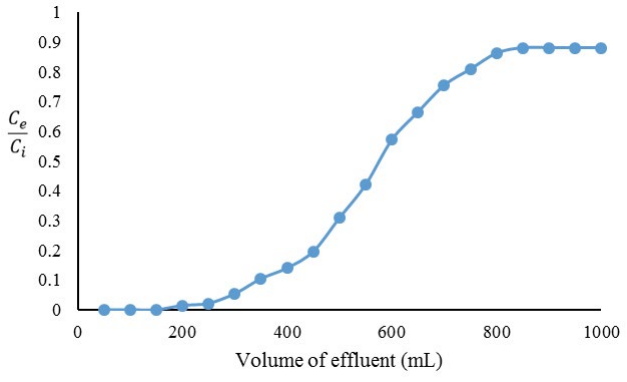

Fig. 5. Breakthrough capacity curve for adsorption of Pb(II) onto lupin straw.

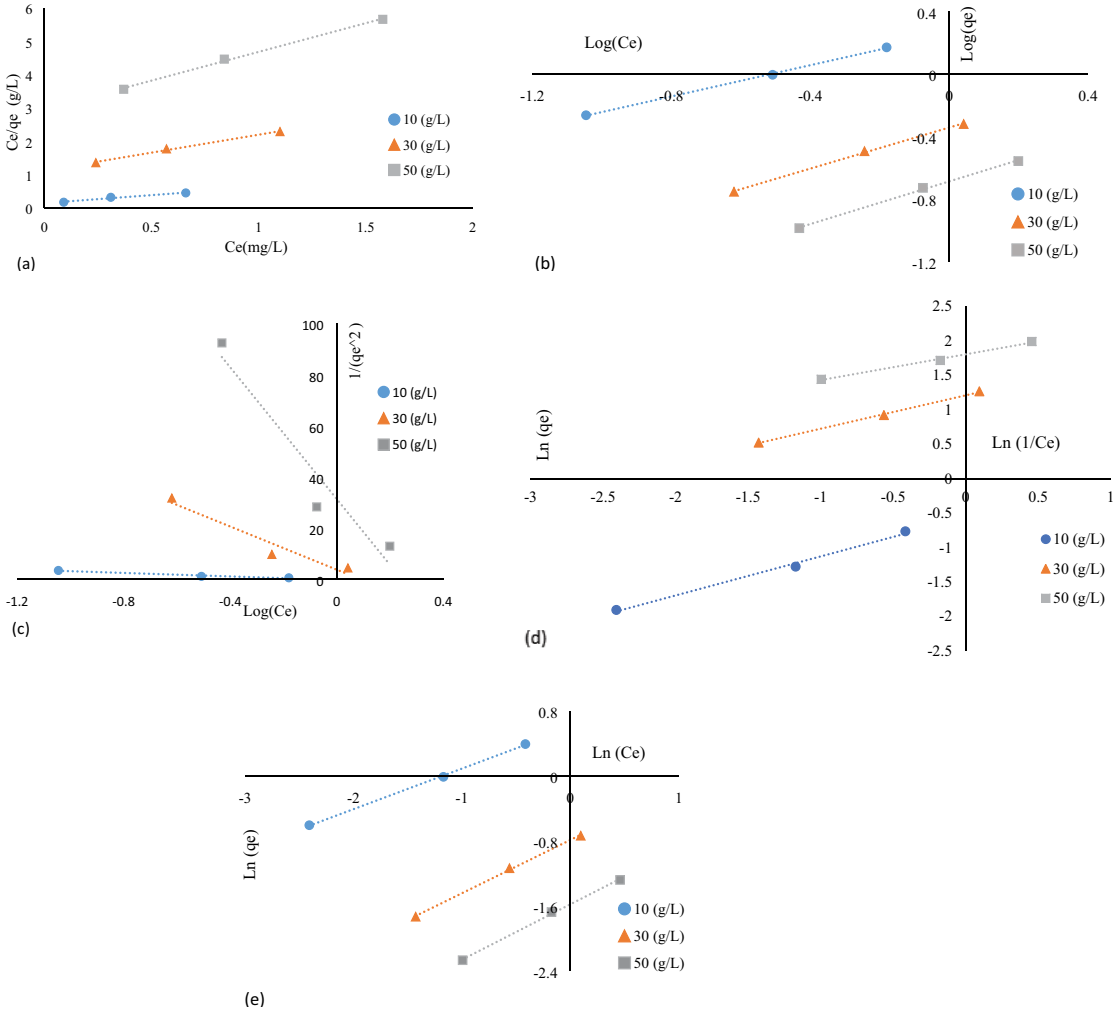

Fig. 6. Langmuir (a), Freundlich (b), Harkins–Jura (c), Redlich–Peterson (d), and Halsey isotherm (e) plots for Pb(II) removal using lupin straw at different adsorbent dosage.

Table 5
Parameters of the Langmuir and the Freundlich isotherm models for lead adsorption onto lupin straw

Adsorbent dosage	Langmuir				Freundlich			
(g/L)	b_L (L/mg)	Q_0 (mg/g)	R_L	r^2	$1/n_f$	K_f	Q_e (mg/g)	r^2
10	3.498	2.085	0.018	0.9734	0.499	1.813	7.135	0.9992
30	0.965	0.929	0.062	0.9951	0.656	0.457	2.770	0.9988
50	0.584	0.579	0.099	0.9976	0.682	0.207	1.346	0.9983

models, the Halsey isotherm indicates higher correlation coefficient (r^2) values. The Halsey isotherm shows a similar correlation coefficient (r^2) to the Freundlich isotherm. Fitting of the experimental data to the Freundlich and the Halsey isotherm equations indicates the heterogeneous and heteroporous nature of lupin straw [69]. In Table 6 the β values, which are obtained by trial and error, are not close to unity concluding that the isotherms are approaching the Freundlich more than Langmuir isotherm.

Fig. 7 shows the Freundlich isotherm validation linear plot where q_e is the equilibrium capacity obtained from the experimental results and q_f is the predicted adsorption capacity calculated from the Freundlich isotherm.

Table 7 shows the comparison of the adsorption capacity of lupin straw, and various agricultural waste adsorbents. Lupin straw sequestrated a significant percentage of lead ion (98.2%) with higher adsorption capacity than the other bio-sorbents.

Table 6
Parameters of the Harkins–Jura, Redlich–Peterson and Halsey isotherm models for lead adsorption onto lupin straw

Adsorbent dosage	Harkins–Jura			Redlich–Peterson				Halsey		
(g/L)	A_H	B_H	r^2	β	A_R	B_R	r^2	N_H	K_H	r^2
10	0.292	–0.111	0.960	0.5663	4.89	0.569	0.9938	2.000	3.287	0.9992
30	0.024	0.085	0.933	0.4864	1.99	3.357	0.9987	1.523	0.304	0.9988
50	0.008	0.242	0.931	0.3756	1.47	6.081	0.9943	1.465	0.099	0.9983

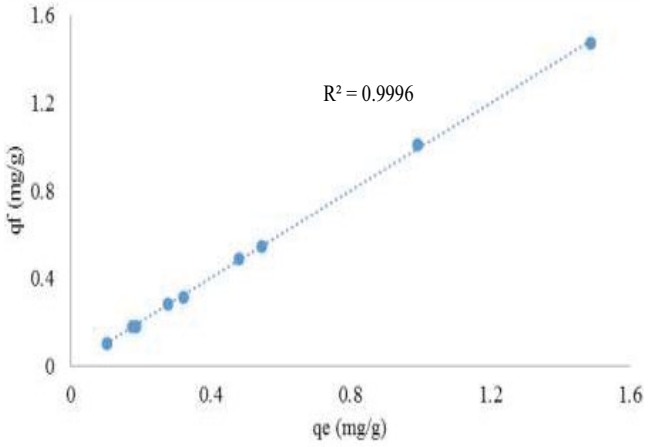

Fig. 7. Freundlich isotherm validation.

Table 7
Adsorption capacities of different agricultural waste adsorbents

Bio-sorbent	Maximum adsorption capacity (mg/g)	Reference
Lupin straw	7.135	This study
Coca shell	6.23	[70]
Olive stone	6.39	[71]
Date stem	5.15	[72]
Barley straw	4.64	[73]
Gmelina arborea leaves	4.6	[74]
Militia ferruginea plant leaves	3.3	[75]
Hazelnut shell	1.78	[76]

4.6.2. Adsorption kinetics study

Five different adsorption kinetic models are proposed to investigate the dynamic mechanism of lead adsorption over time. The best fit kinetic model was observed to be the pseudo-second-order based on the correlation coefficients (r^2). The linear plots of log (q_e–q_t) vs. time were analyzed for pseudo-first-order to obtain adsorption kinetic constant parameters. For the pseudo-second-order kinetic model, the linear data plots of t/q_t against time were used to determine the kinetic constants. The constant values and correlation coefficients of the pseudo-first-order and pseudo-second-order for all lead concentrations are shown in Table 8. Fig. 8 exhibits the pseudo-first-order and pseudo-second-order linear plots.

Elovich, intra-particle diffusion, and fractional power kinetic data plots of lupin straw are shown in Fig. 9. To calculate the constant values of the Elovich, intra-particle diffusion, and fractional power kinetics, linear forms of q_t vs. ln (t), q_t against $t^{1/2}$, and ln (q_t) vs. ln (t) are plotted, respectively.

The constant values and correlation coefficients of the Elovich, intra-particle diffusion, and fractional power kinetic models for varied adsorbate concentrations are shown in Table 9.

The amount of lead ions adsorbed on lupin straw surface at different initial adsorbate concentrations was calculated using the pseudo-second-order, Elovich, and intra-particle diffusion kinetic models over time. Fig. 10 shows the comparison between these calculated data and the experimental data.

According to the parameters obtained from different kinetic models, fitting the lead adsorption process into the pseudo-second-order kinetic model indicates that the adsorption process was a chemical adsorption involving valence forces [77]. In addition, the contribution of intra-particle diffusion of the lead ions and lupin straw surface into the adsorption process was observed.

Table 8
Pseudo-first-order and pseudo-second-order constant values and correlation coefficients of lead removal using lupin straw

Adsorbate concentration (mg/L)	Experimental data	Pseudo-first-order kinetic model		Pseudo-second-order kinetic model		
	q_e	k_f	r^2	k_S	q_e	r^2
5	0.548	0.034	0.976	2.291	0.551	0.9997
10	0.994	0.039	0.9829	1.144	1.002	0.9997
15	1.488	0.044	0.9925	0.655	1.504	0.9997

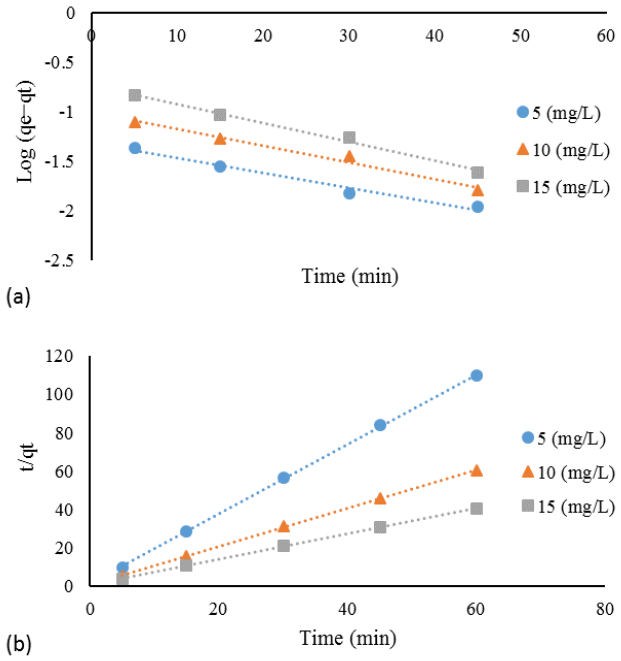

Fig. 8. Pseudo-first-order (a) and pseudo-second-order (b) kinetic plots of lead ions adsorbed onto lupin straw.

5. Conclusion

Lupin straw was studied for its efficiency as a low-cost natural adsorbent to remove dissolved Pb^{2+} ions from synthetic wastewater. This study demonstrated that lupin straw is an economical, nontoxic, and effective adsorbent for the removal of lead from aqueous solutions. Based on the experimental data described above, lupin straw demonstrated a high extraction capacity of 98.4% toward Pb(II) at pH 5.5 and initial adsorbate concentration 5 mg/L. The adsorption process was initially quick and subsequently slowed until it reached equilibrium after 60 min. The breakthrough and exhaustive capacities were found to be 10.98 and 20.16 mg/g, respectively. The experimental data were evaluated by different isotherm models developed by Langmuir, Freundlich, Harkins–Jura, Redlich–Peterson and Halsey. The experimental data fit well into Freundlich and Halsey isotherms equations with high correlation coefficients (r^2 > 0.998), which indicated that the surface of lupin straw was heterogeneous, and multilayer adsorption accrued. From the Freundlich

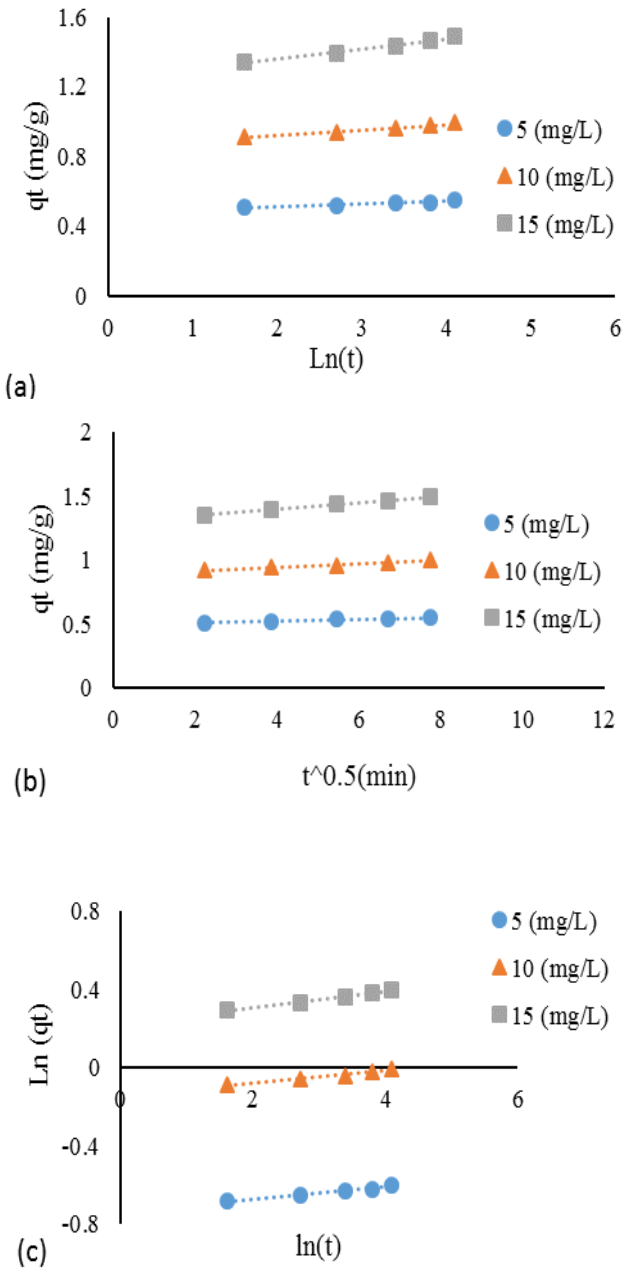

Fig. 9. Elovich (a), intra-particle diffusion (b), and fractional power (c) kinetic plots of lead ions adsorbed onto lupin straw.

Table 9
Elovich, intra-particle diffusion, and fractional power constant values and correlation coefficients of lead removal using lupin straw

Adsorbate concentration	Elovich kinetic model			Intra-particle diffusion kinetic model			Fractional power kinetic model		
(mg/L)	α	β	r^2	K_i	C_i	r^2	ε	ω	r^2
5	0.477	0.016	0.9775	0.007	0.4897	0.9839	0.479	0.031	0.9805
10	0.862	0.031	0.9676	0.014	0.8843	0.9969	0.865	0.032	0.9718
15	1.246	0.057	0.9885	0.026	1.2898	0.9948	1.254	0.041	0.9914

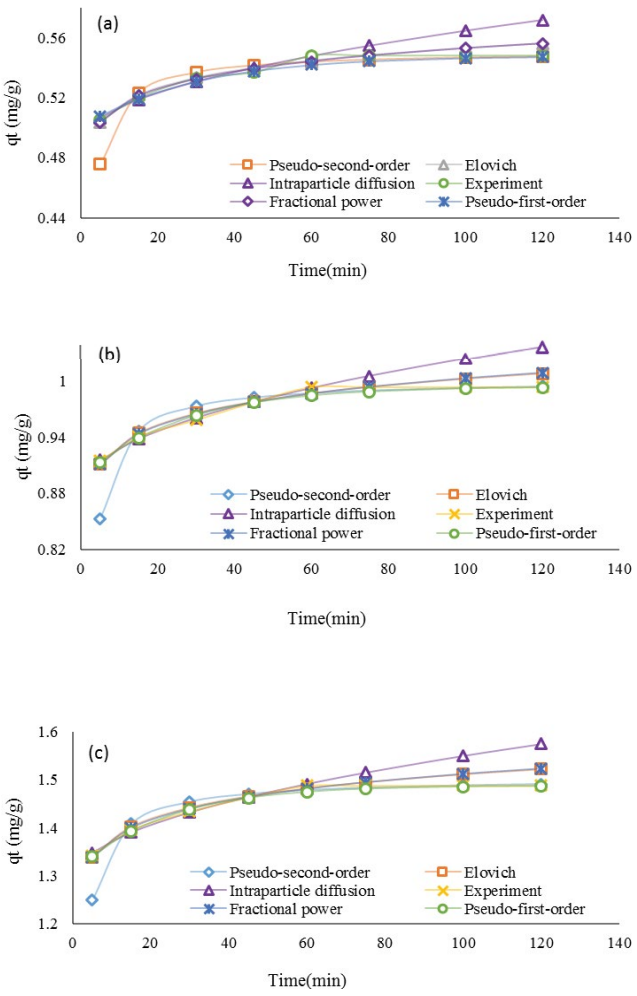

Fig. 10. Amount of lead ions adsorbed over time at initial adsorbate concentrations of 5 (a), 10 (b), and 15 (c) mg/L using the pseudo-second-order, Elovich, intra-particle diffusion, fractional power, pseudo-first-order, and experimental data.

isotherm model, the maximum adsorption capacity of lupin straw was calculated to be 7.1352 mg/g at 23°C. The kinetic studies revealed that the best fit kinetic model was the pseudo-second-order model. Based on the results obtained from the experiment, the process of lead adsorption by lupin straw could be described as chemisorption via chemical functional groups on the adsorbent surface followed by some ion exchange and physical interactions.

Acknowledgements

The authors thank the Faculty of Engineering, Edith Cowan University for funding this project. The author would like to thank Dr Yong Sun at ECU Water and Environmental Research laboratory for technical support.

References

[1] J. Duruibe, M. Ogwuegbu, J. Egwurugwu, Heavy metal pollution and human biotoxic effects, Int. J. Phys. Sci., 2 (2007) 112–118.
[2] World Health Organization, Inter-Organization Programme For the sound Management of Chemicals, Principles and methods for the assessment of risk from essential trace elements, World Health Organization, 2002.
[3] K. Kadirvelu, K. Thamaraiselvi, C. Namasivayam, Removal of heavy metals from industrial wastewaters by adsorption onto activated carbon prepared from an agricultural solid waste, Bioresour. Technol., 76 (2001) 63–65.
[4] A. El-Said, Biosorption of Pb (II) ions from aqueous solutions onto rice husk and its ash, J. Am. Sci., 6 (2010) 143–150.
[5] H. Hu, R. Shih, S. Rothenberg, B.S. Schwartz, The epidemiology of lead toxicity in adults: measuring dose and consideration of other methodologic issues, Environ. Health Persp., 115 (2007) 455.
[6] A. Gholami, A. Moghadassi, S. Hosseini, S. Shabani, F. Gholami, Preparation and characterization of polyvinyl chloride based nanocomposite nanofiltration-membrane modified by iron oxide nanoparticles for lead removal from water, J. Ind. Eng. Chem., 20 (2014) 1517–1522.
[7] J. Song, H. Oh, H. Kong, J. Jang, Polyrhodanine modified anodic aluminum oxide membrane for heavy metal ions removal, J. Hazard. Mater., 187 (2011) 311–317.
[8] S. Parsons, Advanced Oxidation Processes for Water and Wastewater Treatment, IWA Publishing, 2004.
[9] Y. Zhang, L. Yan, W. Xu, X. Guo, L. Cui, L. Gao, Q. Wei, B. Du, Adsorption of Pb (II) and Hg (II) from aqueous solution using magnetic $CoFe_2O_4$-reduced graphene oxide, J. Mol. Liq., 191 (2014) 177–182.
[10] M. Iqbal, A. Saeed, S.I. Zafar, FTIR spectrophotometry, kinetics and adsorption isotherms modeling, ion exchange, and EDX analysis for understanding the mechanism of Cd^{2+} and Pb^{2+} removal by mango peel waste, J. Hazard. Mater., 164 (2009) 161–171.
[11] M. Naushad, A. Mittal, M. Rathore, V. Gupta, Ion-exchange kinetic studies for Cd (II), Co (II), Cu (II), and Pb (II) metal ions over a composite cation exchanger, Desal. Wat. Treat., 54 (2015) 2883–2890.
[12] S. Theepharaksapan, C. Chiemchaisri, W. Chiemchaisri, K. Yamamoto, Removal of pollutants and reduction of biotoxicity in a full scale chemical coagulation and reverse osmosis leachate treatment system, Bioresour. Technol., 102 (2011) 5381–5388.
[13] M.G. Khedr, Radioactive contamination of groundwater, special aspects and advantages of removal by reverse osmosis and nanofiltration, Desalination, 321 (2013) 47–54.
[14] X. Deng, L. Lü, H. Li, F. Luo, The adsorption properties of Pb (II) and Cd (II) on functionalized graphene prepared by electrolysis method, J. Hazard. Mater., 183 (2010) 923–930.
[15] S.L. Cort, Methods for Removing Heavy Metals from Water Using Chemical Precipitation and Field Separation Methods, in, Google Patents, 2005.
[16] R.J. Gohari, W. Lau, T. Matsuura, E. Halakoo, A. Ismail, Adsorptive removal of Pb (II) from aqueous solution by novel PES/HMO ultrafiltration mixed matrix membrane, Sep. Purif. Technol., 120 (2013) 59–68.
[17] Z. Thong, G. Han, Y. Cui, J. Gao, T.-S. Chung, S.Y. Chan, S. Wei, Novel nanofiltration membranes consisting of a sulfonated pentablock copolymer rejection layer for heavy metal removal, Environ. Sci. Technol., 48 (2014) 13880–13887.
[18] R. Hilliges, A. Schriewer, B. Helmreich, A three-stage treatment system for highly polluted urban road runoff, J. Environ. Manage., 128 (2013) 306–312.
[19] M. Khiadani, M. Zarrabi, M. Foroughi, Urban runoff treatment using nano-sized iron oxide coated sand with and without magnetic field applying, J. Environ. Health Sci., 11 (2013) 43.
[20] Y.-X. Ma, Y.-L. Kou, D. Xing, P.-S. Jin, W.-J. Shao, X. Li, X.-Y. Du, P.-Q. La, Synthesis of magnetic graphene oxide grafted polymaleicamide dendrimer nanohybrids for adsorption of Pb (II) in aqueous solution, J. Hazard. Mater., (2017) 407–416.
[21] B. Guo, F. Deng, Y. Zhao, X. Luo, S. Luo, C. Au, Magnetic ion-imprinted and–SH functionalized polymer for selective removal of Pb (II) from aqueous samples, Appl. Surf. Sci., 292 (2014) 438–446.

[22] A.O. Dada, F.A. Adekola, E.O. Odebunmi, Kinetics, mechanism, isotherm and thermodynamic studies of liquid phase adsorption of Pb^{2+} onto wood activated carbon supported zerovalent iron (WAC-ZVI) nanocomposite, Cogent Chem., 3 (2017) 1351653.
[23] O. Karnitz, L.V.A. Gurgel, J.C.P. De Melo, V.R. Botaro, T.M.S. Melo, R.P. de Freitas Gil, L.F. Gil, Adsorption of heavy metal ion from aqueous single metal solution by chemically modified sugarcane bagasse, Bioresour. Technol., 98 (2007) 1291–1297.
[24] L. Cutillas-Barreiro, R. Paradelo, A. Igrexas-Soto, A. Núñez-Delgado, M.J. Fernández-Sanjurjo, E. Álvarez-Rodriguez, G. Garrote, J.C. Nóvoa-Muñoz, M. Arias-Estévez, Valorization of biosorbent obtained from a forestry waste: competitive adsorption, desorption and transport of Cd, Cu, Ni, Pb and Zn, Ecotoxicol. Environ. Saf., 131 (2016) 118–126.
[25] E. Pehlivan, T. Altun, S. Parlayıcı, Utilization of barley straws as biosorbents for Cu^{2+} and Pb^{2+} ions, J. Hazard. Mater., 164 (2009) 982–986.
[26] P. Senthil Kumar, C. Senthamarai, A. Sai Deepthi, R. Bharani, Adsorption isotherms, kinetics and mechanism of Pb (II) ions removal from aqueous solution using chemically modified agricultural waste, Canadian J. Chem. Eng., 91 (2013) 1950–1956.
[27] B. Volesky, Z. Holan, Biosorption of heavy metals, Biotechnol. Progr., 11 (1995) 235–250.
[28] S. Babel, T.A. Kurniawan, Low-cost adsorbents for heavy metals uptake from contaminated water: a review, J. Hazard. Mater., 97 (2003) 219–243.
[29] A. Demirbas, Heavy metal adsorption onto agro-based waste materials: a review, J. Hazard. Mater., 157 (2008) 220–229.
[30] S. Suganya, A. Saravanan, P. Senthil Kumar, M. Yashwanthraj, P. Sundar Rajan, K. Kayalvizhi, Sequestration of Pb (II) and Ni (II) ions from aqueous solution using microalga *Rhizoclonium hookeri*: adsorption thermodynamics, kinetics, and equilibrium studies, J. Water Reuse Desal., 7 (2017) 214–227.
[31] J. Anwar, U. Shafique, M. Salman, A. Dar, S. Anwar, Removal of Pb (II) and Cd (II) from water by adsorption on peels of banana, Bioresour. Technol., 101 (2010) 1752–1755.
[32] R. Mallampati, L. Xuanjun, A. Adin, S. Valiyaveettil, Fruit peels as efficient renewable adsorbents for removal of dissolved heavy metals and dyes from water, ACS Sustain. Chem. Eng., 3 (2015) 1117–1124.
[33] R. Zein, R. Suhaili, F. Earnestly, E. Munaf, Removal of Pb (II), Cd (II) and Co (II) from aqueous solution using *Garcinia mangostana* L. fruit shell, J. Hazard. Mater., 181 (2010) 52–56.
[34] G.F. Coelho, A.C. Gonçalves Jr, C.R.T. Tarley, J. Casarin, H. Nacke, M.A. Francziskowski, Removal of metal ions Cd (II), Pb (II), and Cr (III) from water by the cashew nut shell *Anacardium occidentale* L, Ecol. Eng., 73 (2014) 514–525.
[35] A. Babarinde, G.O. Onyiaocha, Equilibrium sorption of divalent metal ions onto groundnut (*Arachis hypogaea*) shell: kinetics, isotherm and thermodynamics, Chem. Int., 2 (2016) 3.
[36] P. Senthil Kumar, Adsorption of lead (II) ions from simulated wastewater using natural waste: a kinetic, thermodynamic and equilibrium study, Environ. Progr. Sustain. Energy, 33 (2014) 55–64.
[37] B. Singha, S.K. Das, Removal of Pb (II) ions from aqueous solution and industrial effluent using natural biosorbents, Environ. Sci. Pollut. Res., 19 (2012) 2212–2226.
[38] U.A. Gilbert, I.U. Emmanuel, A.A. Adebanjo, G.A. Olalere, Biosorptive removal of Pb^{2+} and Cd^{2+} onto novel biosorbent: defatted *Carica papaya* seeds, Biomass Bioenergy, 35 (2011) 2517–2525.
[39] K. Jayaram, M. Prasad, Removal of Pb (II) from aqueous solution by seed powder of *Prosopis juliflora* DC, J. Hazard. Mater., 169 (2009) 991–997.
[40] M.M. Ibrahim, W.W. Ngah, M. Norliyana, W.W. Daud, M. Rafatullah, O. Sulaiman, R. Hashim, A novel agricultural waste adsorbent for the removal of lead (II) ions from aqueous solutions, J. Hazard. Mater., 182 (2010) 377–385.
[41] H. Lalhruaitluanga, K. Jayaram, M. Prasad, K. Kumar, Lead (II) adsorption from aqueous solutions by raw and activated charcoals of *Melocanna baccifera* Roxburgh (bamboo)—a comparative study, J. Hazard. Mater., 175 (2010) 311–318.
[42] E. Gunasundari, S. Kumar, Adsorption isotherm, kinetics and thermodynamic analysis of Cu (II) ions onto the dried algal biomass (*Spirulina platensis*), J. Ind. Eng. Chem., 56 (2017) 129–144.
[43] I. Langmuir, The constitution and fundamental properties of solids and liquids. Part I. Solids, J. Am. Chem. Soc., 38 (1916) 2221–2295.
[44] H. Freundlich, Über die adsorption in lösungen, Z. Phys. Chem., 57 (1907) 385–470.
[45] K. Singh, S. Hasan, M. Talat, V. Singh, S. Gangwar, Removal of Cr (VI) from aqueous solutions using wheat bran, Chem. Eng. J., 151 (2009) 113–121.
[46] N.K. Amin, Removal of direct blue-106 dye from aqueous solution using new activated carbons developed from pomegranate peel: adsorption equilibrium and kinetics, J. Hazard. Mater., 165 (2009) 52–62.
[47] C.A. Başar, Applicability of the various adsorption models of three dyes adsorption onto activated carbon prepared waste apricot, J. Hazard. Mater., 135 (2006) 232–241.
[48] Y.-S. Ho, G. McKay, Pseudo-second order model for sorption processes, Process Biochem., 34 (1999) 451–465.
[49] M. Rauf, M. Iqbal, I. Ellahi, S. Hasany, Kinetic and thermodynamic aspects of ytterbium adsorption on sand, Adsorpt. Sci. Technol., 13 (1996) 97–104.
[50] F.-C. Wu, R.-L. Tseng, R.-S. Juang, Initial behavior of intraparticle diffusion model used in the description of adsorption kinetics, Chem. Eng. J., 153 (2009) 1–8.
[51] M. Low, Kinetics of Chemisorption of Gases on Solids, Chem. Rev., 60 (1960) 267–312.
[52] S. Chien, W. Clayton, Application of Elovich equation to the kinetics of phosphate release and sorption in soils, Soil Sci. Soc. Am. J., 44 (1980) 265–268.
[53] R. Dalal, Desorption of soil phosphate by anion-exchange resin, Commun. Soil Sci. Plant Anal., 5 (1974) 531–538.
[54] A. Dada, J. Ojediran, A.P. Olalekan, Sorption of from aqueous solution unto modified rice husk: isotherms studies, Adv. Phys. Chem., 2013 (2013).
[55] M.-C. Popescu, C.-M. Popescu, G. Lisa, Y. Sakata, Evaluation of morphological and chemical aspects of different wood species by spectroscopy and thermal methods, J. Mol. Struct., 988 (2011) 65–72.
[56] T. Kondo, The assignment of IR absorption bands due to free hydroxyl groups in cellulose, Cellulose, 4 (1997) 281–292.
[57] D.H.K. Reddy, K. Seshaiah, A. Reddy, M.M. Rao, M. Wang, Biosorption of Pb^{2+} from aqueous solutions by *Moringa oleifera* bark: equilibrium and kinetic studies, J. Hazard. Mater., 174 (2010) 831–838.
[58] R. Han, L. Zhang, C. Song, M. Zhang, H. Zhu, L. Zhang, Characterization of modified wheat straw, kinetic and equilibrium study about copper ion and methylene blue adsorption in batch mode, Carbohydr. Polym., 79 (2010) 1140–1149.
[59] C.-M. Popescu, M.-C. Popescu, G. Singurel, C. Vasile, D.S. Argyropoulos, S. Willfor, Spectral characterization of eucalyptus wood, Appl. Spectrosc., 61 (2007) 1168–1177.
[60] M. Rafatullah, O. Sulaiman, R. Hashim, A. Ahmad, Adsorption of copper (II), chromium (III), nickel (II) and lead (II) ions from aqueous solutions by meranti sawdust, J. Hazard. Mater., 170 (2009) 969–977.
[61] M. Poletto, A.J. Zattera, R. Santana, Structural differences between wood species: evidence from chemical composition, FTIR spectroscopy, and thermogravimetric analysis, J. Appl. Polym. Sci., 126 (2012) E337–E334.
[62] M. Fan, D. Dai, B. Huang, Fourier Transform Infrared Spectroscopy for Natural Fibres, in: Fourier Transform-Materials Analysis, InTech, 2012.
[63] J. Coates, Interpretation of infrared spectra, a practical approach, Enc anal Chem, (2000).
[64] H. Struszczyk, Modification of lignins. III. Reaction of lignosulfonates with chlorophosphazenes, J. Macromol. Sci. Chem., 23 (1986) 973–992.
[65] G.C. Pimentel, C.H. Sederholm, Correlation of infrared stretching frequencies and hydrogen bond distances in crystals, J. Chem. Phys., 24 (1956) 639–641.

[66] M. Haris, K. Sathasivam, The removal of methyl red from aqueous solutions using modified banana trunk fibers, Arch. Appl. Sci. Res., 2 (2010) 209–216.
[67] M. Ghasemi, M. Naushad, N. Ghasemi, Y. Khosravi-Fard, A novel agricultural waste based adsorbent for the removal of Pb (II) from aqueous solution: kinetics, equilibrium and thermodynamic studies, J. Ind. Eng. Chem., 20 (2014) 454–461.
[68] R. Negi, G. Satpathy, Y.K. Tyagi, R.K. Gupta, Biosorption of heavy metals by utilising onion and garlic wastes, Int. J. Environ. Pollut., 49 (2012) 179–196.
[69] C. Song, S. Wu, M. Cheng, P. Tao, M. Shao, G. Gao, Adsorption studies of coconut shell carbons prepared by KOH activation for removal of lead (II) from aqueous solutions, Sustainability, 6 (2013) 86–98.
[70] N. Meunier, J. Laroulandie, J. Blais, R. Tyagi, Cocoa shells for heavy metal removal from acidic solutions, Bioresour. Technol., 90 (2003) 255–263.
[71] G. Blázquez, M. Calero, F. Hernáinz, G. Tenorio, M. Martín-Lara, Equilibrium biosorption of lead (II) from aqueous solutions by solid waste from olive-oil production, Chem. Eng. J., 160 (2010) 615–622.
[72] H. Yazid, R. Maachi, Biosorption of lead (II) ions from aqueous solutions by biological activated dates stems, J. Environ. Sci. Technol., 1 (2008) 201–213.
[73] E. Pehlivan, T. Altun, S. Parlayıcı, Utilization of barley straws as biosorbents for Cu^{2+} and Pb^{2+} ions, J. Hazard. Mater., 164 (2009) 982–986.
[74] J.O. Tijani, M. Musah, I. Blessing, Sorption of Lead (II) and Copper (II) ions from Aqueous Solution by acid modified and unmodified *Gmelina arborea* (Verbenaceae) leaves, J. Emerg. Trends Eng. Appl. Sci., 2 (2011) 734–740.
[75] A.A. Mengistie, T.S. Rao, A.P. Rao, M. Singanan, Removal of lead (II) ions from aqueous solutions using activated carbon from Militia ferruginea plant leaves, Bull. Chem. Soc. Ethiopia, 22 (2008) 3.
[76] G. Cimino, A. Passerini, G. Toscano, Removal of toxic cations and Cr (VI) from aqueous solution by hazelnut shell, Water Res., 34 (2000) 2955–2962.
[77] W. Song, B. Gao, T. Zhang, X. Xu, X. Huang, H. Yu, Q. Yue, High-capacity adsorption of dissolved hexavalent chromium using amine-functionalized magnetic corn stalk composites, Bioresour. Technol., 190 (2015) 550–557.